JGR Biogeosciences

RESEARCH ARTICLE
10.1029/2024JG008308

Seasonal Variation in Flow and Metabolic Activity Drive Nitrate and Carbon Supply and Demand in a Temperate Agricultural Stream

Lukas Hallberg[1,2], **Susana Bernal**[3], **and Magdalena Bieroza**[1]

[1]Department of Soil and Environment, Swedish University of Agricultural Sciences, Uppsala, Sweden, [2]Now at School of Geography, Earth and Environmental Sciences, University of Birmingham, Birmingham, UK, [3]Integrative Freshwater Ecology Group, Centre d'Estudis Avançats de Blanes (CEAB-CSIC), Blanes, Spain

Key Points:

- Supply:demand ratios show that nitrate and dissolved organic carbon supply typically overwhelm biological demand in an agricultural stream
- Evidence for biological nitrate limitation occurred during summer low flow and metabolic peak, despite high nitrate loading on annual term
- Storm events consistently stimulated in-stream ecosystem respiration but suppressed gross primary production

Supporting Information:

Supporting Information may be found in the online version of this article.

Correspondence to:

M. Bieroza,
magdalena.bieroza@slu.se

Citation:

Hallberg, L., Bernal, S., & Bieroza, M. (2024). Seasonal variation in flow and metabolic activity drive nitrate and carbon supply and demand in a temperate agricultural stream. *Journal of Geophysical Research: Biogeosciences*, *129*, e2024JG008308. https://doi.org/10.1029/2024JG008308

Received 18 JUN 2024
Accepted 12 NOV 2024

Author Contributions:

Conceptualization: Lukas Hallberg, Magdalena Bieroza
Data curation: Lukas Hallberg
Formal analysis: Lukas Hallberg, Susana Bernal, Magdalena Bieroza
Funding acquisition: Susana Bernal, Magdalena Bieroza
Methodology: Lukas Hallberg, Susana Bernal, Magdalena Bieroza
Visualization: Lukas Hallberg
Writing – original draft: Lukas Hallberg
Writing – review & editing: Lukas Hallberg, Susana Bernal, Magdalena Bieroza

Abstract In-stream biogeochemical processing, typically associated with base flow conditions, has recently been assessed at higher discharges, aided by high frequency monitoring. However, the potential for nutrient and carbon processing is still largely unknown in streams impacted by agriculture, representing major pathways for eutrophication and diffuse pollution. In this study, we measured solute concentrations and gross primary productivity (GPP) and ecosystem respiration (ER) to infer nitrate (NO_3^-) and dissolved organic carbon (DOC) supply and demand across contrasting hydrological conditions. As expected, solute supply greatly surpassed in-stream biological demand for both NO_3^- and DOC for intermediate to large discharges. However, during four consecutive weeks in summer, lowered NO_3^- supply and high metabolic activity led to a 60% and 31% reduction in stream NO_3^- and DOC export. We also compared metabolism-discharge versus solute concentration-discharge patterns during storm events to better understand biogeochemical responses to high flows. Metabolic rates showed a contrasting response to storm events: ER increased while GPP decreased following declines in NO_3^- concentrations. The positive correlation between GPP and NO_3^- concentrations suggests that GPP suppression can be partially attributed to decreased NO_3^- availability during storm events. This study supports the idea that agricultural streams have a limited capacity to biologically process DOC and NO_3^-. However, it also emphasizes that the balance between supply and demand can vary from severe saturation to limitation, depending on seasonal fluctuations in discharge and metabolic activity, highlighting the crucial role of mitigating pollution at its source during hydrologically active periods to improve water quality.

Plain Language Summary To understand the overall capacity for water-living organisms to reduce downstream export of pollutants (i.e., nitrogen and carbon), it is necessary to measure biological uptake rates (demand) together with pollutant loads (supply) across seasons and varying stream flow. However, the role of biological nitrogen and carbon processing has been less explored in streams impacted by high nutrient inputs from agriculture, especially during higher flows. Based on 2-year monitoring of an agricultural stream, we argue that biological demand plays only a minor and temporary role for reducing nitrogen and carbon exports in these systems, which occurred only during summer when stream flow decreased and biological activity peaked. Although storm events occurred in periods with overall low biological activity, stormflow peaks consistently increased productivity of in-stream bacteria and invertebrates, but decreased productivity of plants and algae. This study supports the idea that biological organisms in agricultural streams have a limited capacity to reduce nitrogen and carbon exports. However, it also shows that biological nitrogen availability can vary from severe saturation to limitation, depending on seasonal differences in stream flow and biological activity.

1. Introduction

Headwater streams represent the primary link between terrestrial and aquatic environments and are therefore pivotal for regulating export of water, matter and energy to and within river networks (Alexander et al., 2007; Dodds & Oakes, 2008). A growing body of research has identified the central role of in-stream biogeochemical processing in transforming and retaining biogenic solutes such as nitrate (NO_3^-) and dissolved organic carbon (DOC), which can impact solute export at the entire stream network scale (Raymond et al., 2016; Seybold & McGlynn, 2018; Wollheim et al., 2018). However, drivers underpinning in-stream biogeochemical processing are highly variable across biomes and hydrological conditions (Bernhardt et al., 2022) and are further complicated by anthropogenic disturbances such as agricultural land uses (Abbott et al., 2018; Royer et al., 2006). Streams

draining agricultural landscapes often show low water residence times induced by channel modification, and are recipients of high NO_3^- and bioavailable DOC inputs from agricultural soils. Yet, our current understanding of the role of in-stream biogeochemical processing in regulating solute exports stems primarily from studies using constant-rate solute experimental additions (Ensign & Doyle, 2006; Mineau et al., 2016; Peterson et al., 2001; Tank et al., 2018). These methods are generally constrained to base flow conditions (Workshop, 1990), which prevents the assessment of in-stream biogeochemical processing during higher discharges and their implications on annual export budgets. Further, estimation of in-stream nutrient uptake using experimental additions is only possible in streams with low nutrient concentrations (Covino et al., 2018), excluding agricultural streams characterized by consistent NO_3^- saturation. Recent developments in sensor technology (Almeida et al., 2014; Bieroza et al., 2023) and stream metabolic modeling from diel variation in dissolved oxygen (O_2) concentrations (Appling et al., 2018) have enabled comparisons of solute inputs (supply) and metabolic solute processing (demand) across different discharges, either by mass balance approach (Bernal et al., 2019; Jarvie, Sharpley, et al., 2018) or by applying stoichiometric principles (Bertuzzo et al., 2022; O'Donnell & Hotchkiss, 2022; Trentman et al., 2022).

In theory, in-stream demand for bioreactive solutes is predicted to increase with supply up to moderate-magnitude storm events (Wollheim et al., 2018). Thus, streams could reduce downstream nutrient and DOC exports across a range of flows, wider than initially assumed. Increased in-stream biogeochemical processing during storms has been observed in semi-natural streams for NO_3^- and to some extent for DOC, demonstrating the key role of solute supply on stream biological demand (Bernal et al., 2019; Demars, 2019; Seybold & McGlynn, 2018). In nutrient-enriched agricultural streams, the contribution of in-stream biogeochemical processing to reduction in solute export during low-to intermediate-flow conditions could be even higher because metabolic rates often exceed those measured in nutrient-poor, low impacted streams (Bernot et al., 2010; Burrell et al., 2014). This applies in particular during biologically active periods when high temperature and open riparian canopies favor both gross primary productivity (GPP) and ecosystem respiration (ER). The potential for biogeochemical processing during higher discharges can be further enhanced by stream remediation, for example, by introducing floodplains in agricultural streams. When storm events occur during growing seasons, it has been shown that floodplain vegetation can support higher reach-scale GPP rates and associated photoautotrophic NO_3^- uptake (Roley et al., 2014). Concerning DOC inputs, agricultural streams often receive more bioavailable fractions derived from the microbial alteration of organic matter processing in agricultural soils (Arango et al., 2008; Bernot et al., 2006; Graeber et al., 2015), which can reduce energy costs for heterotrophic metabolism and thereby enhance stream ER (Fuß et al., 2017). However, the greater demand for NO_3^- and DOC in agricultural streams could be balanced out by the higher supply of these solutes, which consistently surpasses that of pristine systems. As such, our understanding of in-stream NO_3^- and DOC processing with varying hydrological conditions, and its consequences for solute exports, remain limited in agricultural streams (Hill, 2023; Plont et al., 2020). Recent studies that investigate metabolic responses to storm events in nutrient-enriched streams show mixed patterns with both stimulation and suppression in GPP and ER, respectively, exposing significant knowledge gaps concerning underlying drivers (O'Donnell & Hotchkiss, 2022; Trentman et al., 2022). To improve our understanding of the overall impact of agricultural land use on the capacity of streams to regulate downstream solute exports, it is necessary to integrate both solute supply and in-stream biological demand across varying discharges and seasons.

The overall aim of this study was to quantify stream metabolic rates, the associated demand of NO_3^- and DOC, and the supply of these solutes across varying flow conditions, in an agricultural stream with floodplains and riparian canopy. Moreover, we explored the responses to discharge of both metabolic rates and solute concentrations to better understand changes in supply sources and in-stream demand during storm events. Stream metabolic rates and solute demand were estimated by combining diel O_2 time series at the catchment outlet and open-channel modeling with simple stoichiometric principles, while solute supply was estimated from high-frequency sensor monitoring. During the monitoring period (23 months), 21 storm events of different magnitude and duration were identified, allowing for analysis of the response in metabolic rates and solute concentrations to a wide range of discharges. The experimental setting enabled us to address the following questions:

1. What is the biological demand associated with stream metabolic activity across seasons and hydrological conditions in an agricultural stream?
2. Under what environmental conditions can biological demand of NO_3^- and DOC effectively regulate solute downstream export?
3. Are responses in metabolic rates and solute concentrations coupled during storm events?

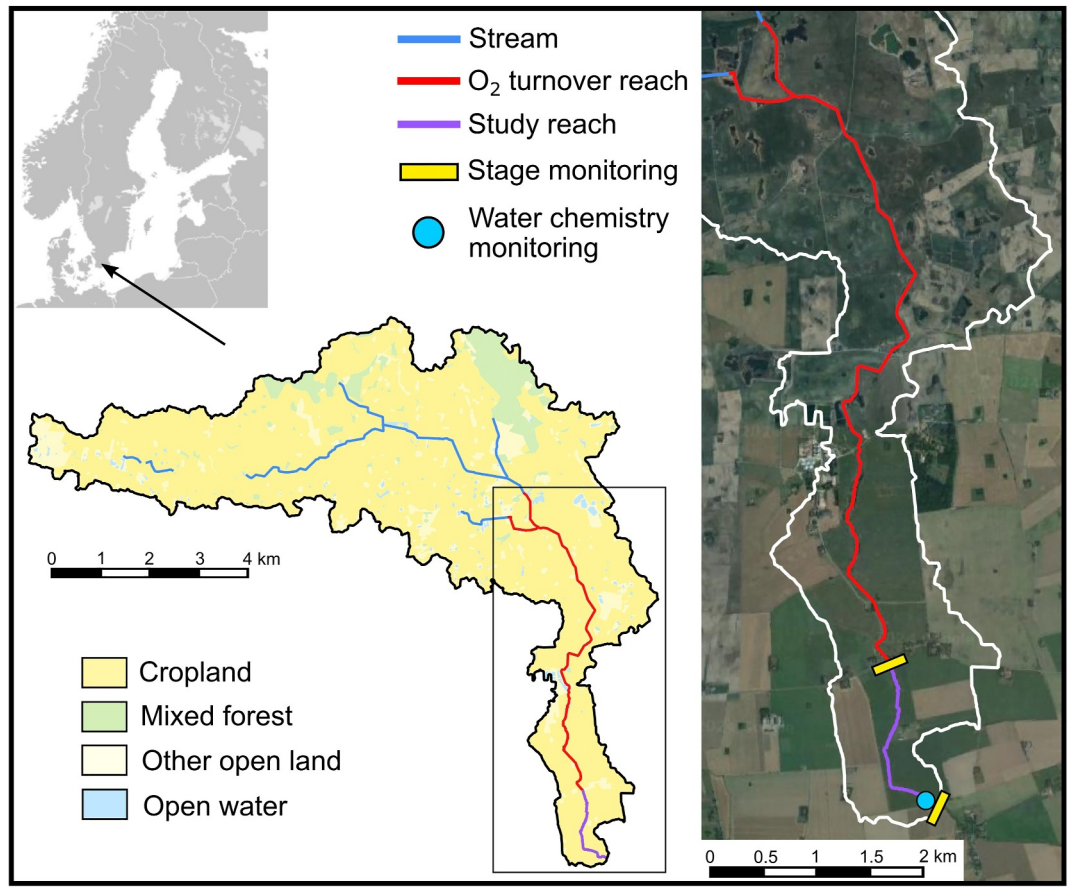

Figure 1. Location of the study catchment and satellite image of land adjacent to the mean oxygen (O_2) turnover reach (red line) and study reach (purple line). Water stage was monitored at endpoints of the study reach (yellow lines) and water chemistry, including dissolved O_2 for metabolism calculations, at the catchment outlet (blue circle). Satellite images: Google, ©2024 Maxar Technologies. Land use maps: ©Lantmäteriet.

We expected solute supply to exert a dominant control on downstream export of NO_3^- and DOC across varying discharges and different seasons, overwhelming the metabolically derived biological processing of these solutes. Moreover, photoautotrophic NO_3^- uptake was predicted to be suppressed by the closed riparian canopy during the growing season and stimulated upon floodplain inundation during higher flows. In contrast, we expected DOC depletion during the growing season when high ER may increase DOC demand.

2. Materials and Methods

2.1. Study Area

Tullstorpsån is a second order stream with low channel slope (0.05%) that drains an agricultural headwater catchment in South Sweden (55.4°N, 13.4°E). The study reach (1.7 km) is delineated by stage and discharge monitoring stations at and up- and downstream, together with a water chemistry monitoring station at downstream (Figure 1). The Tullstorpsån catchment is dominated by limestone bedrock, overlain by quaternary sediments with 20–40 m depth and loam top soils. Land use is dominated by tile-drained arable agricultural land (81%), consisting of winter-sown cereal crops and temporary ley grass cultivation. Throughout the catchment, the main stem of the stream has been subjected to successive restoration measures by local stakeholders (Hedin & Kivi-vuori, 2015), including channel re-meandering (established in 2009 and 2014) and construction of floodplains (established in 2014). In conjunction, riparian vegetation with shrubs and trees were introduced and currently cover >60% of the study reach (Figure 1). A previous macrophyte survey from August 2021 in the study showed an almost 100% cover by *Typha* and *Epilobium* species (Hallberg et al., 2022). Thus, light conditions are impacted both by macrophytes and riparian canopy.

2.2. Data Collection and Processing

Water chemistry monitoring at the study reach consisted of high-frequency measurements of dissolved O_2 and NO_3^--N concentrations, fluorescence emission intensity measured at excitation wavelength 365 nm and emission wavelength 480 nm (fDOM), turbidity and temperature, all recorded with 15 min intervals using a multiparameter sonde (EXO2, YSI) from July 2021 to November 2023. At the same location, water samples were collected monthly from April 2020 to November 2023 and analyzed in laboratory for NO_3^--N (ISO 15923-1:2013), ammonium-nitrogen (NH_4^+-N; ISO 15923-1:2013), DOC (SS-EN 1484) and soluble reactive phosphorus (SRP; ISO 15923-1:2013) with 0.45 µm filtration. High-frequency measurements of water chemistry were corrected according to the procedure in Supporting Information S1. High-frequency fDOM was used to infer DOC concentrations after correcting for temperature and turbidity (Figure S1 in Supporting Information S1). High-frequency NO_3^--N concentrations were calibrated to NO_3^--N concentrations measured in grab water samples (Figure S2 in Supporting Information S1).

Stream discharge (Q) and velocity were estimated every 10 min at the two stage monitoring stations (Figure 1). Stage rating curves were established using paired manual Q and velocity measurements (n = 8–11) and water stage data measured with pressure sensors (Hallberg, Djodjic, & Bieroza, 2024). To analyze hydrological flow regime, base flow index (Gustard et al., 1992) was calculated annually using *baseflows* in R package hydrostats (Bond, 2022). Mean water stage was estimated by dividing wetted cross-section area with stream width of 15 cross-sections measured between the two stage monitoring stations, for subsequent areal scaling of metabolic rates along O_2 turnover lengths (Figure 1). For each cross-section, wetted cross-section area and width were measured for all Q values by establishing linear and non-linear stage rating curves.

Photosynthetic active radiation (PAR) at top of canopy in the downstream location of the reach was retrieved from the Swedish radiation model (STRÅNG; https://strang.smhi.se/), with hourly intervals during the study period. To account for PAR absorption by both riparian canopy overhang and emergent macrophytes that covered the majority of the modeled reach, daily stream surface PAR was estimated by subtracting PAR absorbed by vegetation from top of canopy PAR (Figure S3 in Supporting Information S1).

2.3. Stream Metabolism Modeling

High-frequency time series of O_2, stream surface light, water temperature and mean depth were used to estimate daily stream metabolism rates from July 2021 to November 2023, excluding summer months in 2022 due to sensor malfunction. Daily GPP, ER and gas transfer coefficient ($K_{600;}$ day^{-1}) were estimated with a one-station method (Odum, 1956), using a Bayesian hierarchical model from streamMetabolizer R package and model structure *b_Kb_oipi_tr_plrckm.stan* (Appling et al., 2018). The one-station approach was chosen since the spatial heterogeneity was relatively minor along the O_2 turnover length (Chapra & Di Toro, 1991; Reichert et al., 2009). The main sources of spatial heterogeneity were groundwater inputs from tile drainage (see below), differences in bed channel substrates and a confluence with a tributary draining small wetlands, located 10 km upstream of the monitoring station (Figure 1). The channel bed consisted of gravel substrates 0–5 km upstream from the monitoring location, while fine benthic organic matter dominated further upstream. The change in substrates suggests that hyporheic exchange was likely more pronounced in the downstream section with gravel bed, which could potentially increase the influence of groundwater upwelling. The distance to the confluence was exceeded by daily O_2 turnover lengths on 154 days out of 622 modeled days, mainly coinciding with periods of high flows during storms. The daily O_2 turnover length was estimated as three times water velocity divided by K_{600}. The model was specified to account for both observation and process error and K_{600} was constrained to Q (by daily pooling) to reduce equifinality among GPP, ER and K_{600} when fitted to daily O_2 curves. Default model probability priors were used to estimate K_{600} and compared against K_{600} estimated from hydraulic geometry, following Equations 1 and 2 in Raymond et al. (2012; Figure S4a in Supporting Information S1).

Daily lateral water inputs along the study reach were estimated from mean daily differences in Q between the upstream and downstream stage monitoring stations. On average, lateral water inputs contributed 30% to stream Q during flows below the 55th percentile (Q < 0.2 m^3 s^{-1}). This corresponds to conditions wherein tile drains contribute to the majority of lateral inputs and deep groundwater with low O_2 concentrations is disconnected from surface water (Rozemeijer et al., 2010; Thomas et al., 2016). During most of the storm events, we could not accurately assess the water balance between the two stage monitoring stations due to uncertainties in stage-rating relationships. Although we cannot rule out an increase in groundwater inputs during storm events, the observed

dilution of NO_3^- and stable supply of DOC suggests that shallow pathways (i.e., tile drainage) with limited exposure to both nitrogen and O_2-consuming soil processes, were likely the main contributors to stream runoff (Burns et al., 2019). Modeled GPP and ER were validated by removing estimates with biologically impossible values (GPP < 0 and ER > 0), poor model convergence (R-hat > 1.2) or lack of fit between daily observed and modeled O_2 ($r^2 < 0.6$ or $0.4 < r^2 < 0.6$ and root mean square error (RMSE < 0.1; Table S1 in Supporting Information S1). This resulted in 650 days selected for further analysis, from a total of 719 days. In addition, the occurrence of equifinality was assessed by regressing ER and K_{600} (Figure S4b in Supporting Information S1), where a lack of correlation indicates few potential combinations GPP, ER and K_{600} values and good model accuracy. There was no indication of equifinality either for the entire modeled period or during storm events (Figure S4c in Supporting Information S1).

2.4. Estimating Supply and Demand of NO_3^- and DOC

To investigate in-stream biological processing of NO_3^- and DOC inputs, and its effect on downstream exports, we estimated NO_3^--N and DOC supply and demand as solute mass per benthic area and day. Supply and demand were compared across the entire study period and in the growing season 2023 (1st April to 31st August). The growing season was defined as the top of canopy PAR > 75 W m^{-2}, which coincides with the onset of GPP increase in spring. Supply was calculated according to King et al. (2014) as:

$$S_{\text{supply}} = \frac{QC}{wL} \quad (1)$$

where S_{supply} is daily solute flux (g m^{-2} day^{-1}), Q is discharge (L s^{-1}), C is solute concentration (mg L^{-1}), w is stream width (m) and L is daily O_2 turnover length (m). Given the relatively low average depth (0.19 ± 0.01 m) of the studied reach, we assumed complete vertical mixing of solutes. Note that S_{supply} represents the loading of solutes to the same reach from which the metabolic signal is generated. To test if solute loadings were generated from lengths equal to or greater than O_2 turnover lengths, daily solute spiraling length (S_w; m) was calculated as:

$$S_w = \frac{QC}{S_{\text{demand}} w} \quad (2)$$

where S_{demand} is the biological solute demand (g m^{-2} day^{-1}; see calculation below). For all measured days, $S_w > O_2$ turnover lengths for both NO_3^- and DOC. Thus, the areal solute loadings were considered to be persistent along entire O_2 turnover lengths.

Biological NO_3^- and DOC demand (S_{demand}) was estimated by combining metabolic rates with simple stoichiometric principles. S_{demand} was scaled to g m^{-2} day^{-1} for comparison with supply. All nitrogen (N) uptake was assumed be in the form of NO_3^-, as NO_3^--N corresponded to 94 ± 9% of dissolved inorganic nitrogen concentrations between July 2021 and November 2022, and NH_4^+-N concentration was low (average = 0.08 ± 0.03 mg L^{-1}). Since NO_3^- demand was inferred from O_2-derived metabolic rates, we assumed that it includes assimilatory uptake by photoautotrophs and aerobic heterotrophs, but does not account for dissimilatory N pathways.

To estimate photoautotrophic NO_3^- uptake, we first derived net primary production by determining the slope of the 90th percentile of GPP regressed against ER to subtract photoautotrophic respiration from GPP (Hall & Beaulieu, 2013). Net primary production was converted to inorganic carbon (C) fixation using the photosynthetic quotient of 1.1, assuming a balance between photorespiration and O_2 release from NO_3^- assimilation (Trentman et al., 2023). A stoichiometric C:N ratio of 12 was then used to convert C to photoautotrophic NO_3^--N uptake (Webster et al., 2003). In its turn, heterotrophic DOC and NO_3^--N demand were estimated from heterotrophic respiration rates (ER—photoautotrophic respiration), since photoautotrophic respiration is not affecting NO_3^- and DOC turnover. Heterotrophic respiration was converted to C using the respiratory quotient of 1 (Bernal et al., 2022) and to NO_3^--N by assuming 0.2 bacterial growth efficiency (del Giorgio & Cole, 1998) and a C:N ratio of five of heterotrophic bacteria (Fenchel et al., 2012). The flowchart of these calculations is provided in Figure S5 in Supporting Information S1.

The balance between solute supply and demand was analyzed by comparing the supply:demand ratio over time. Since we did not measure solute saturation kinetics, we could not test the onset of solute limitation directly. Yet, we considered that a supply:demand ratio <1 was indicative of near limitation conditions.

To validate estimates of biological NO_3^- demand, daytime NO_3^- deficit was calculated from hourly means of high-frequency NO_3^- concentrations (Heffernan & Cohen, 2010; Equation 2). Hourly NO_3^- deficit from NO_3^- maxima (nighttime) was calculated for each hour of the day and aggregated to NO_3^- fluxes (g m^{-2} day^{-1}). NO_3^- maxima was calculated as an interpolated baseline of NO_3^- maxima at preceding and subsequent nights (night maxima was identified between 21:00 and 04:00). Positive NO_3^- deficit values indicate lower NO_3^- concentrations during daytime, which can be attributed to photoautotrophic uptake. These NO_3^- fluxes were compared to those obtained from modeled metabolic rates using the coefficient of determination (r^2) and RMSE.

2.5. Solute and Metabolism Response to Storm Events

Hydrological storm events were identified with sensor measurements, based on base flow separation by using a Lyne-Hollick filter in the R package hydrostats (Bond, 2022). We defined storm events as an increase of $Q > 100\%$, compared to base flow, and with a Q peak > 0.2 m^3 s^{-1}. Events with multiple peaks were classified as one event if Q minima on the falling limb did not drop below <100% of base flow.

To explore solute and metabolic behavior during storm events, we used concentration-discharge (C-Q) and metabolism-discharge (M-Q) metrics to describe the direction (hysteresis index [HI]; Lloyd et al., 2015) and magnitude of change (response index [RI], also referred to as flushing index for solutes by Butturini et al., 2008). For each storm event, the two indices were calculated for NO_3^--N and DOC concentrations measured at 15 min intervals, and for GPP and absolute ER rates (|ER|) measured at daily intervals. Moreover, we explored C-Q relationships for turbidity (FNU), which was used as a proxy for suspended solids, to partition physical from biogeochemical effects on stream metabolic responses. Events with missing concentrations (1, 7, and 14 in Figure 1) or poor model accuracy of metabolic rates (10 and 20 in Figure 1) were excluded from the analysis.

Prior to calculation of HI, water chemistry and metabolic parameters and Q were normalized for each event (Lloyd et al., 2015). The HI describes the direction of change in concentration (or metabolic rate) between the rising and falling limbs of a given event (i.e., clockwise or anti-clockwise) and the size of the hysteresis loop, calculated as:

$$\mathrm{HI}_{Qi} = C,M_{\mathrm{RL\_}Qi} - C,M_{\mathrm{FL\_}Qi}, \tag{3}$$

where HI_{Qi} is the index at percentile i of Q, $C,M_{\mathrm{RL\_}Qi}$ is the normalized concentration (or metabolic rate) on the rising limb of percentile i of Q and $C,M_{\mathrm{RL\_}Qi}$ is the normalized concentration (or metabolic rate) on the falling limb of percentile i of Q. For each event, HI_{Qi} was calculated for every fifth percentile (0.05…0.95) of Q. The mean HI of each event was summarized by averaging HI of all considered percentiles. Values $0.1 < \mathrm{HI} < 1$ denote clockwise behavior, while values $-1 < \mathrm{HI} < -0.1$ denote anti-clockwise behavior. With clockwise patterns, concentrations or metabolic rates increase more rapidly than Q on the rising limb, whereas anti-clockwise patterns imply a delayed concentration or metabolic rate peak compared to Q. Concerning solute concentrations, the direction of HI suggests either the activation of proximal (clockwise) or distal sources (anti-clockwise). The same applies for turbidity. In the case of metabolic rates, clockwise patterns indicate rapid stimulation (alleviation of light, energy or nutrient limitation) upon storm onset while anti-clockwise patterns suggest initial suppression (limitation of light, energy or nutrients) and/or delayed stimulation. Further, we considered that values $-0.1 < \mathrm{HI} < 0.1$ suggest a linear response in concentrations or metabolic rates to Q. To determine the magnitude of change during storm events, we used a RI developed for water chemistry, here defined for both solute concentrations and metabolic rates as:

$$\mathrm{RI} = \frac{C,M_{\mathrm{peak}} - C,M_{bf}}{C,M_{\mathrm{max}}} \tag{4}$$

where C,M_{peak} is the concentration (or metabolic rate) at the event peak, C,M_{bf} is the concentration (or metabolic rate) at the onset of event (base flow) and C,M_{max} is the highest of the two values C,M_{peak} and C,M_{bf}. Solute (or particulate) accretion and metabolism stimulation occur at values $0.1 < \mathrm{RI} < 1$ while solute (or particulate)

dilution or metabolism suppression at values $-1 < RI < -0.1$. We assumed no change in concentration or metabolic response at values $-0.1 < RI < 0.1$.

2.6. Statistical Data Analysis

Environmental drivers of GPP and ER were explored with multiple linear regression, using a best subsets approach (R package leaps; Lumley, 2020). Predictors considered were daily means of Q, light (stream surface PAR), water temperature, NO_3^--N and DOC concentrations and turbidity. Predictor variables were centered and scaled to allow for in-between comparison of regression coefficients. The presence of collinearity was tested with variance inflation factor using *vif* (R package regclass; Petrie, 2020). These statistical analyses were constrained to the growing season in 2023 (1st April to 31st August) when stream metabolic rates were expected to be the highest.

To explore relationships between storm event responses in metabolic rates and solute concentrations, respective RI values were compared against peak Q of events. Further, Spearman rank correlations were tested for both RI and HI values between metabolic rates and solute concentrations. All statistical analyses were performed in R version 4.2.1 (RStudio Team, 2022).

3. Results

3.1. Hydrochemistry and Stream Metabolism Patterns

Hydrology showed distinct seasonality with low flows during summer and autumn, followed by elevated base flow and storm events during winter and spring (Figure 2). Stream Q at the downstream stage station ranged between <0.01 and 5.76 $m^3\ s^{-1}$, wherein base flows on average accounted for 29 ± 3% of annual Q. Stream NO_3^--N concentration averaged 3.90 ± 3.09 mg N L^{-1} and followed the seasonal pattern of Q, with high concentration during periods of hydrological connectivity in winter and spring and low concentration during low flows of summer and autumn (Figure 2). Stream SRP concentration also exhibited a seasonal pattern, but minima occurred early in spring and preceded NO_3^--N minima (Figure S6 in Supporting Information S1). Stream DOC concentration averaged 11.31 ± 2.39 mg L^{-1} and peaked during winter, but showed no direct coupling to hydrology. By contrast, turbidity correlated to Q ($r^2 = 0.57$, $p < 0.01$), averaging 18.93 ± 41.78 FNU across the study period and 4.15 ± 3.75 FNU during base flow.

The stream was net heterotrophic, with mean NEP <0 (−1.92 ± 1.79 g O_2 m^{-2} day^{-1}). Yet, metabolic activity, especially GPP, increased during spring and summer 2023 when PAR exceeded 75 W m^{-2}, resulting in stream autotrophy with NEP peaking at 4.93 g O_2 m^{-2} day^{-1} (Figure 2). During this period, GPP and ER accounted for 89% and 61% of cumulative daily metabolic rates in 2023, respectively (excluding December due to missing data). The daily turnover length of dissolved O_2 averaged 9.3 ± 13.5 km (Figure 1) for the entire study period.

During the growing season, best subsets of multiple linear regression models explained 52% and 65% of variation in GPP and ER rates, respectively (Table 1). In the GPP model, PAR and DOC were the most influential predictors for GPP, which increased with PAR and decreased with DOC. In the ER model, water temperature, GPP and Q showed a positive correlation on ER rates. In contrast, NO_3^--N concentration was negatively correlated.

3.2. NO_3^- and DOC Supply and Demand Patterns

Overall, NO_3^--N and DOC supply greatly surpassed biological demand across intermediate to high Q (Figure 3). The supply:demand ratio increased with Q from 0.5 to 559.8 and from 5.6 to 3,223.3 for NO_3^--N and DOC, respectively. During the growing season 2023, biological NO_3^--N uptake peaked, while NO_3^--N supply decreased as a consequence of low Q (<0.1 $m^3\ s^{-1}$). Consequently, supply:demand ratios decreased to values < 1 during 32 days in May and June 2023 (Figure 4a). During the same period, the concurrent peak in biological DOC uptake also reduced DOC supply:demand ratios but not <1, explained by the more stable supply of DOC compared to NO_3^--N. The increase in photoautotrophic NO_3^--N uptake was substantially higher (111 ± 129%) than the observed daytime removal NO_3^--N concentrations between April and June 2023 (Figure 4b). The reduction in DIN:SRP molar ratio below Redfield ratio of 16:1 during the growing season further suggested a switch from P to N limitation (Figure S6 in Supporting Information S1). During June 2023, biological uptake contributed to the reduction of 60 ± 4% and 31 ± 5% of daily NO_3^--N and DOC mass export, respectively.

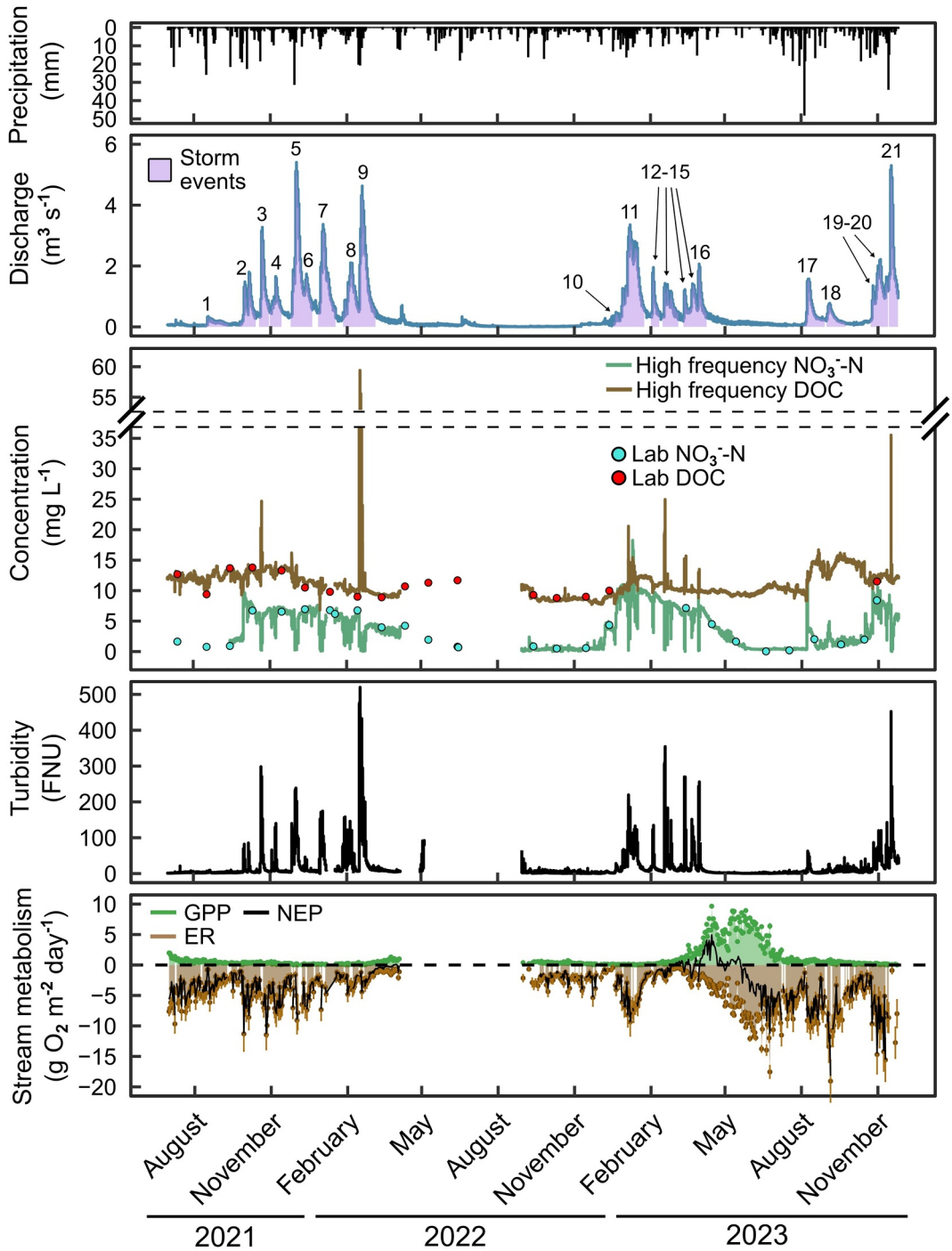

Figure 2. Time series of hydrology, NO_3^--N and dissolved organic carbon concentrations, turbidity and stream metabolism rates in the studied stream between July 2021 and November 2023. Storm events are shown as purple area under discharge. GPP = gross primary production, ER = ecosystem respiration and NEP = net ecosystem production.

3.3. Metabolic and Water Chemistry Responses to Storm Events

The storm event durations were in general long, averaging 14 ± 7 days. The metabolic signal during these events was characterized by high ER (−4.6 ± 3.2 g O_2 m^{-2} day^{-1}), and low GPP (0.5 ± 0.7 g O_2 m^{-2} day^{-1}). The response of daily GPP and ER rates to storm events showed an opposite pattern, with suppression of GPP (negative RI) and stimulation of ER (positive RI; Figure 5). Yet, there was no relationship between event

Table 1
Best Subset Regression of Models Explaining the Variability of Gross Primary Production (GPP) and Ecosystem Respiration (|ER|) Rates During the Growing Season 2023

Selected predictor	Scaled β-value	p-value	VIF
GPP (g O_2 m^{-2} day^{-1})			
PAR	0.44	<0.01	1.16
DOC	−0.34	<0.01	1.80
$Temp_{water}$	−0.16	0.05	1.98
Q	−0.09	0.24	1.64
Adjusted R^2		0.52	
Model p-value		<0.01	
|ER| (g O_2 m^{-2} day^{-1})			
$Temp_{water}$	0.71	<0.01	4.39
GPP	0.63	<0.01	1.42
Q	0.38	<0.01	2.15
NO_3^--N	−0.34	<0.01	5.64
Adjusted R^2		0.65	
Model p-value		<0.01	

Note. Predictors considered were: discharge (Q), stream surface photosynthetic active radiation (PAR), water temperature, nitrate-nitrogen (NO_3^--N), dissolved organic carbon (DOC) and turbidity. GPP was also used as a predictor in the model with ER as response. Predictors are sorted by regression coefficient (β-value). Variance inflation factor (VIF) values <5 indicate absence of collinearity.

magnitude and metabolic rates (Figure 5), indicating that events up to 5 m^3 s^{-1} could stimulate ER. In fact, ER rates increased during 18 out of 19 storm events, demonstrating that hydrological disturbance rather stimulated than disrupted heterotrophic activity. The concomitant suppression of GPP resulted in a more net heterotrophic stream during storm events. The average HI of GPP and ER ranged between −0.1 and 0.1, indicating that changes in metabolic rates and Q were synchronous with Q (Figure 5).

The response of NO_3^--N concentrations to storm events was dominated by RI < −0.1 (12 out 17 events), indicating limited NO_3^--N supply. This behavior was further corroborated by the decrease in RI with increasing Q peak (Figure 5). DOC concentrations showed an overall neutral response regardless of Q peak, characterized by −0.1 < RI < 0.1 (11 out of 21 events). Only 7 events showed RI > 0.1 for DOC. Turbidity showed strong accretion during events, RI increased up to storm events with Q peak = 2 m^3 s^{-1} where it reached a plateau. On average, both NO_3^--N and DOC concentrations showed negative HI (anti-clockwise hysteresis), with average HI similar to that of ER. This pattern indicates that responses in both solutes and ER were slightly delayed in relation to Q peak of events. By contrast, turbidity was dominated by positive HI (clockwise hysteresis; Figure 5).

Values of RI for GPP and NO_3^--N concentrations were correlated to each other, suggesting that GPP was more suppressed during storms showing greater NO_3^--N dilution (Figure 6a). By contrast, values of RI for GPP were not correlated with RI values of either DOC concentration or turbidity. RI values for ER were not correlated with RI values of either DOC concentration (Figure 6b), NO_3^--N concentration or turbidity. Further, HI values of GPP and ER were not correlated to those of either NO_3^--N concentration, DOC concentration or turbidity, which indicated that the timing of response of metabolic rates and solutes to storm events was uncoupled.

4. Discussion

4.1. Drivers of Metabolic Regime in an Agricultural Stream With Closed Canopy

Agricultural streams usually lack a well-developed riparian canopy, though this is becoming an increasingly common feature in restored reaches, such as the one in this study. We found that riparian shading supported net heterotrophy in the study stream (ER > GPP), and that GPP:ER ratios were comparable to those reported for closed canopy streams across the USA (Bernhardt et al., 2022). Moreover, we found that light availability was the primary control of GPP, suggesting that riparian phenology was controlling the temporal dynamics of stream photoautotrophs. However, we lacked an open stream comparison and could not assess to which extent stream shading actually affected in-stream GPP and associated biological demand. The benefits of restoring riparian zones in agricultural streams are still under debate. Shading can provide a range of water quality benefits, such as interception of lateral nutrient and sediment inputs, increased biodiversity, improved ecological status and buffering of water temperatures (Burdon et al., 2020; Burrell et al., 2014). However, closed canopies can also restrict GPP and associated NO_3^- assimilation (Bernot et al., 2006; Tank et al., 2018) and thereby limit their capacity to regulate nutrient exports. Accordingly, we were unable to directly attribute the effect of NO_3^- concentrations to responses in GPP due to coinciding light limitations. In the best subset GPP model, NO_3^--N concentration was excluded as explanatory variable due to low predictive power. Besides the light control of GPP, there was a negative relationship between GPP and DOC, which was likely an indirect effect of delayed DOC mineralization of primary producer biomass, occurring after GPP declined (Bertilsson & Jones, 2003). If the sole aim is to maximize NO_3^- uptake during summer periods, open canopies and enhanced GPP might be more beneficial. However, this can lead to proliferation of toxic algae (Burrell et al., 2014), and an overall decrease in aquatic ecosystem functioning and higher sensitivity to impacts from higher temperatures. When predicting ER, water temperature and GPP were identified as the most important drivers, which are both dependent on light availability and thus canopy cover. Interestingly, DOC concentration did not explain ER as it was excluded in the

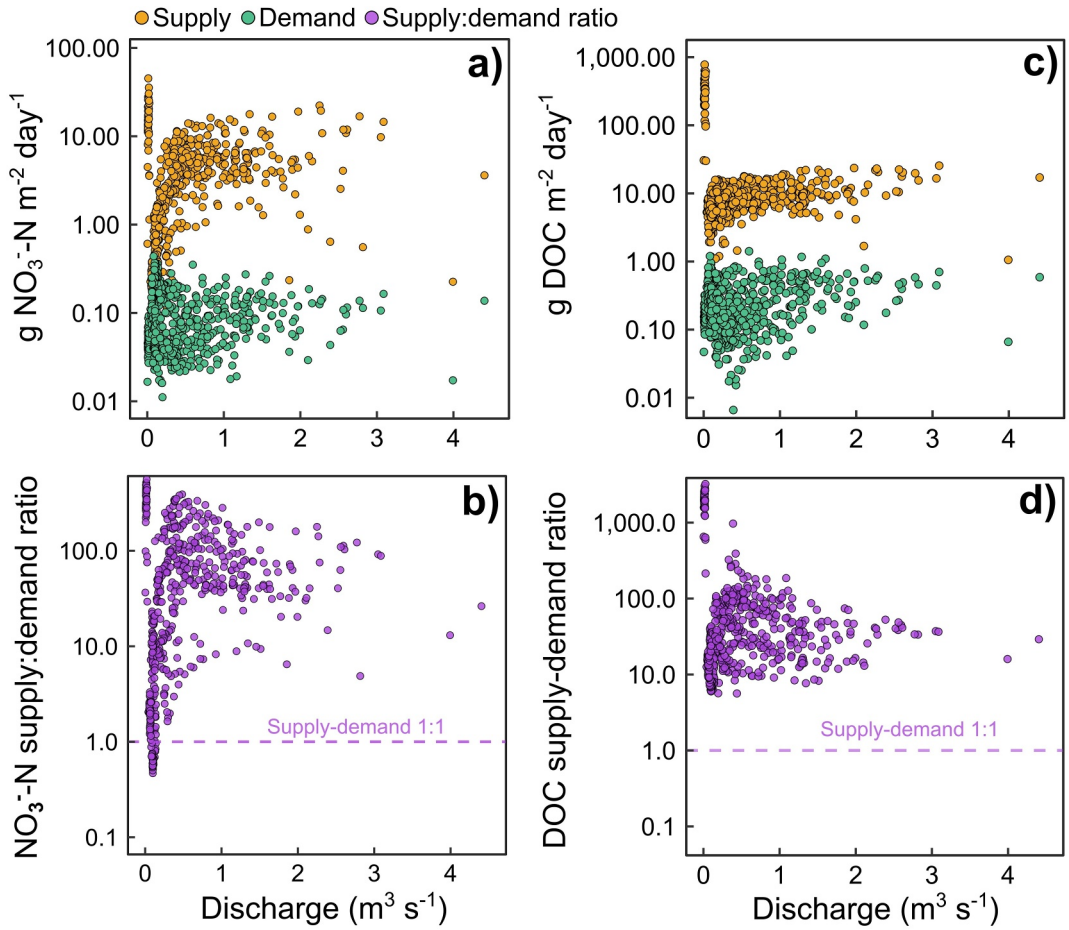

Figure 3. Mean daily values of solute supply, demand and the supply:demand ratios of (a), (b) NO_3^--N and (c), (b) dissolved organic carbon, compared to discharge values.

best subset ER model. This suggests that ER was stimulated by labile organic carbon provided from photoautotrophs rather than in-stream bulk DOC that comprise a mix of terrestrial and aquatic sources with differing bioavailability (Bertuzzo et al., 2022; Descy et al., 2002). Thus, riparian canopy cover can also play an important role in regulating ER and associated carbon fluxes during the growing season.

4.2. Interplay Between Solute Supply and Demand

In accordance with our expectation, we found that daily NO_3^- and DOC supply consistently overwhelmed biological demand during most of the study period (23 months) in this agricultural headwater stream. During intermediate to high discharges ($Q > 0.1$ m^3 s^{-1}), biological processing in the study stream was insufficient to substantially store or transform either NO_3^- or DOC inputs, which contrasts with the higher in-stream processing capacity reported for small and intermediate storms in pristine streams (Bernal et al., 2019; Seybold & McGlynn, 2018). Although the uncertainty in supply estimates increased with flow, the overall pattern of supply >> demand was maintained across the 90% confidence intervals of estimated flow. The negligible role of stream metabolic activity to regulate NO_3^- and DOC concentrations during most of the year and across hydrological conditions is consistent with previous observations in agriculturally impacted streams (Frankforter et al., 2010; Preiner et al., 2020). This pattern clearly diverges from the theoretical behavior that predicts coupling between supply and demand up to moderate storm events (Wollheim et al., 2018), suggesting that in streams with high nutrient loads, such as those draining agricultural catchments, coupling between supply and demand might be constrained to low flow periods.

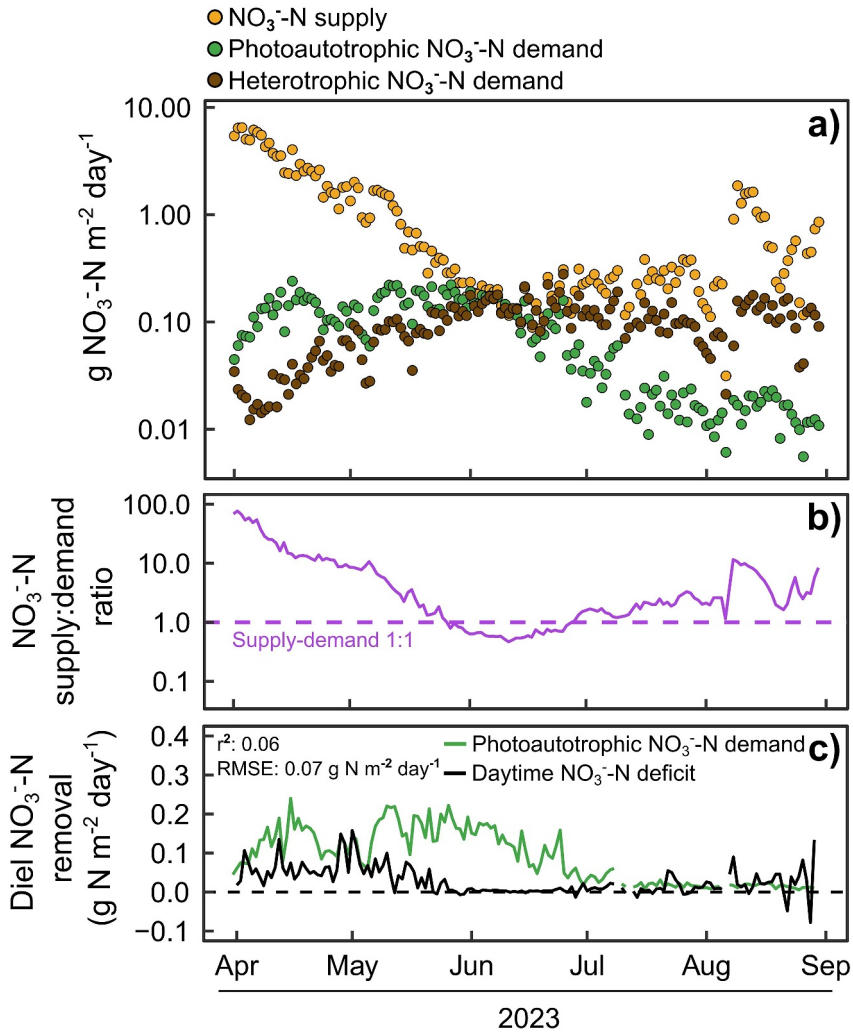

Figure 4. Temporal patterns of (a) daily NO_3^--N supply (orange circles), NO_3^--N demand by photoautotrophs (green circles) and heterotrophs (brown circles), and (b) supply:demand ratio (purple solid line) during the growing season 2023. (c) Photoautotrophic NO_3^--N demand (U_{Aut}; green line) compared to daytime NO_3^--N deficit (NO_{3def}; black line) based on high-frequency NO_3^--N concentrations. Goodness-of-fit between U_{Aut} and NO_{3def} are evaluated with coefficient of determination (r^2) and root mean square error. The dashed black line shows no concentration changes between daytime and nighttime.

In contrast to the expectation that floodplain connectivity contributes to increased biological NO_3^- demand, supply:demand ratios for NO_3^- did not decline during the onset of floodplain inundation. This result can be partially explained because periods of floodplain inundation ($Q > 0.67$ m^3 s^{-1}) at the study stream were accompanied by high solute supply, occurring when GPP was light limited (PAR < 75 W m^{-2}). In contrast, Roley et al. (2014) showed that floodplain inundation, coinciding with sufficient light availability, contributed to increased GPP rates in a similar agricultural stream reach, compared to a channelized reach. Likewise, floodplain connectivity could increase NO_3^- removal through denitrification (Hallberg et al., 2022; Roley et al., 2012; Speir et al., 2020), though this process could not be identified with our approach. Overall, the suppression of GPP and the relatively low magnitude of ER compared to solute supply suggests that metabolic activity during high flows was insufficient to substantially decrease NO_3^- and DOC fluxes to downstream ecosystems, despite hydrological connectivity to vegetated floodplains.

Although we used fixed literature values of photosynthetic and respiratory quotients when estimating NO_3^- and DOC demand from metabolic rates, we note that these quotients can differ across systems and thereby affect the accuracy of demand derived from metabolism (Bernal et al., 2022; Trentman et al., 2023). Other in-stream

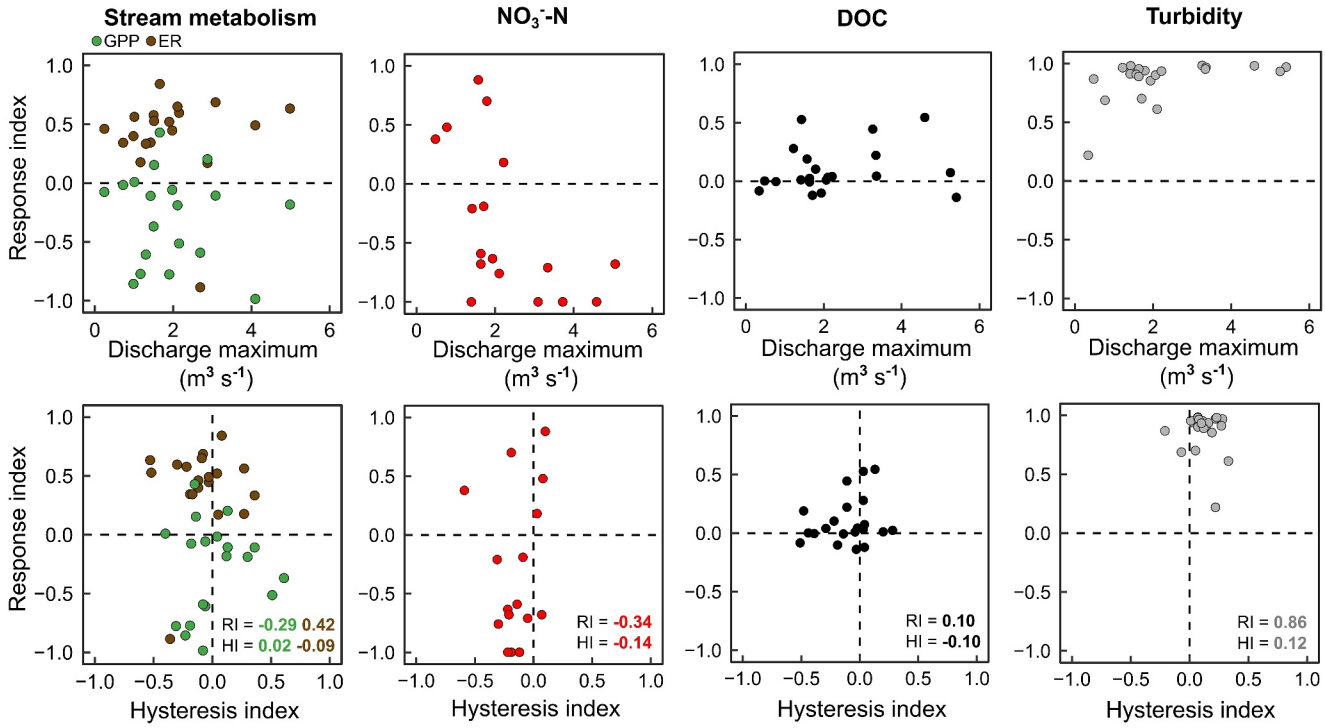

Figure 5. Distribution of storm event responses of stream metabolic rates (gross primary production (GPP) and ecosystem respiration (ER)), NO_3^--N, dissolved organic carbon (DOC) and turbidity. For each storm events, the response index (RI) is compared against discharge maximum (top panels) and hysteresis index (HI) (bottom panels). Stream metabolism includes 19 events; NO_3^--N 17 events; DOC and turbidity 21 events. GPP and ER were analyzed at daily intervals and solutes (and turbidity) at 15 min intervals. Means of RI and HI are shown within panels.

biogeochemical processes not captured by diel O_2 cycles might also be operating within the study reach, for instance, denitrification and nitrification for NO_3^-, and photochemical oxidation and geochemical sorption for DOC. Therefore, we might be underestimating the biological demand of these solutes to some extent. An unknown proportion of ER (previously reported range 0.01–0.11 g O_2 m^{-2} day^{-1}; Duff et al., 2008; Webster et al., 2003) can be derived from nitrification that releases NO_3^-. However, this process is balanced against NO_3^- removal by denitrification. Jarvie, Sharpley, et al. (2018) showed that the ratio of nitrification:denitrification rates can be affected by NEP: when NEP > 1, higher O_2 concentrations (>8 mg L^{-1}) led to net nitrification while during NEP < 1, denitrification surpassed nitrification rates. However, in our study, NEP < 1 did not result in O_2 concentrations indicative of the favoring of denitrification over nitrification, neither during the growing season (7.70 ± 2.39 mg O_2 L^{-1}) nor winter seasons (10.86 ± 1.96 mg O_2 L^{-1}). This demonstrates that in well-aerated

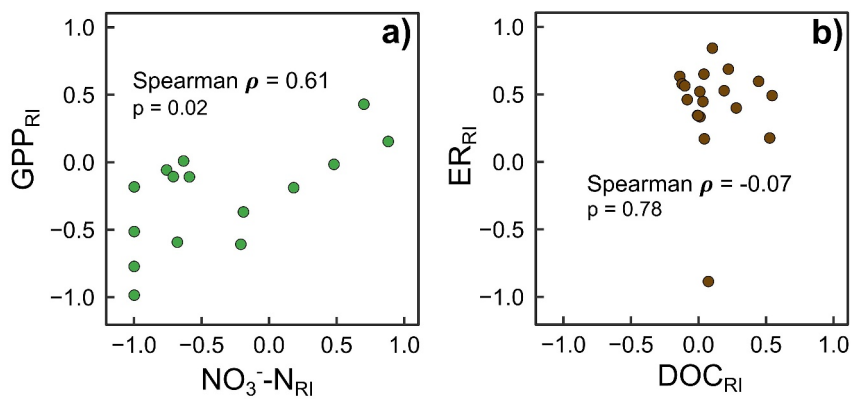

Figure 6. Correlation between response index of (a) gross primary production and NO_3^--N, and (b) ecosystem respiration and dissolved organic carbon. Spearman rank coefficients (ρ) and p-values are shown within panels.

streams, nitrification and associated production of NO_3^- can still dominate among dissimilatory nitrogen pathways despite net heterotrophy.

4.3. Evidence of NO_3^- Limitation During the Growing Season

The combined peak in GPP and decline in NO_3^- supply during the growing season 2023 suggests a month-long period of relatively high NO_3^- uptake when demand clearly surpassed the supply of this nutrient. This pattern could even lead to NO_3^- limitation given that observed DIN:SRP ratios decreased clearly below the Redfield ratio (16:1; Mebane et al., 2021; Redfield, 1958). The asynchronous patterns exhibited by NO_3^- and SRP concentrations further accentuated NO_3^- limitation during this period. The lack of correlation between observed daytime NO_3^- deficits and photoautotrophic NO_3^- removal inferred from metabolic rates was partially explained by the onset of NO_3^- limitation. Supply:demand ratios <1 resulted in the cessation of diel NO_3^- cycling but the delayed decline in photoautotrophic NO_3^- demand suggests that primary producers' N storage capacity and plasticity in biomass stoichiometry can buffer the lack of in-stream NO_3^- supply (Appling & Heffernan, 2014). Hence, photoautotrophic activity was maintained up to a month after the onset of NO_3^- limitation. We also note that daytime NO_3^- deficits may have been influenced by the co-occurrence of diel processes that dampen NO_3^- removal, such as nitrification and N mineralization, which could explain the overall lower removal rates compared to photoautotrophic uptake from metabolic rates. For instance, positive correlations between daily NO_3^- and O_2 concentrations were observed during 30 days between May and August, suggesting the dominance of nitrification over NO_3^- assimilation. During the growing season, higher metabolic activity also resulted in a decrease in supply:demand ratios of DOC down to 1.5, which excludes the occurrence of carbon limitation. The higher supply:demand ratios of DOC compared to NO_3^- was explained by the more stable supply of DOC throughout the growing period, which was likely sufficient to satisfy the heterotrophic carbon demand. During biologically active periods, transient nutrient limitation commonly occurs in pristine headwater streams (Gibson et al., 2015; Mulholland, 2004; Tank et al., 2018) but is rarely observed in anthropogenically impacted streams receiving high NO_3^- inputs (Jarvie, Smith, et al., 2018; von Schiller et al., 2008). The occurrence of NO_3^- limitation in this study was therefore unexpected, demonstrating that nutrient limitation in agricultural headwater streams is not solely restricted to NH_4^+ and SRP, as previously reported (Arango et al., 2008; Bernot et al., 2006).

On the other hand, in-stream NO_3^- demand inferred from metabolic activity was too low (supply:demand ratio >50) to account for the reduction in NO_3^- supply observed at the onset of the growing season. We reason that biological NO_3^- demand of both agricultural crops and floodplain vegetation likely played an important role in reducing stream NO_3^- concentrations. Although floodplain vegetation without inundation does not directly impact on water column GPP signal, it could indirectly influence stream NO_3^- concentrations by removing this nutrient from interstitial pore water (Qian et al., 2021). In addition, NO_3^- assimilation by in-stream emergent macrophytes may also have contributed to NO_3^- removal in the water column. Our metabolic model considered that only submerged compartments of macrophytes contributed to in-stream GPP (Pastor et al., 2023). However, given the abundance of emergent macrophytes in the study reach, it is reasonable to assume that this biotic compartment also contributed to NO_3^- assimilation, since a share of their photosynthesis occurred aerially above the water column. A remediation strategy to reduce remineralization of NO_3^- and DOC stored in vegetation is to cut and remove biomass from floodplain and stream, in the window after GPP peak and before plant senescence. However, precautions should be taken, especially for macrophyte cutting, as higher cutting frequencies have been linked to impaired ecological status in the ecosystems (Baattrup-Pedersen et al., 2018).

4.4. Divergent Responses in Metabolism, NO_3^- and DOC During Storm Events

Storm events affected the stream metabolism by consistently decreasing the NEP through ER stimulation and GPP suppression. A negative response in GPP to storm events has been confirmed in previous studies (O'Donnell & Hotchkiss, 2022; Trentman et al., 2022), attributed to scouring of benthic and suspended autotrophs and light attenuation by suspended solids. Moreover, our results suggest that GPP suppression can result from decreased NO_3^- availability because GPP decreased with decreasing NO_3^- concentrations during storm events. Decreased NO_3^- concentrations in conjunction with expected increases in P concentrations could result in lower N:P ratios that have been shown to limit phytoplankton growth (Kelly et al., 2019). The extension of O_2 turnover lengths during storm flows may have increased the contribution from the upstream tributary draining small wetlands, which could potentially increase GPP due to increased autotrophy in flow-through wetlands draining agricultural soils (Maynard et al., 2012). However, a previous synthesis (Hoellein et al., 2013) showed that wetland metabolic

rates usually are comparable to those measured in streams. In addition, the confluence was located 10 km upstream from the monitoring station, and thus, its influence on the measured metabolic rates might be fairly limited. The consistent stimulation of ER measured during storms contrasts with previous studies reporting either stimulation, suppression or neutral responses (Bertuzzo et al., 2022; O'Donnell & Hotchkiss, 2022; Trentman et al., 2022). We acknowledge that our results should be taken with caution given the unknown contribution of groundwater inputs during increasing flow. From the 21 monitored storms, we could verify gaining conditions in only two cases (15 and 16; Figure 2), for which groundwater contributed up to 50% of stream flow. Following the approach of Hall and Tank (2005), and assuming 5% lower groundwater O_2 concentrations compared to stream water, modeled |ER| rates would have been reduced by 52 ± 26% compared to estimates without considering groundwater inputs. This means that we might be overestimating ER during some storm events, though the direction of response persisted, thus indicating that ER was stimulated with increasing flow. Note that the GPP estimates using the one-station approach are unaffected by groundwater O_2 inputs (assuming stable input across day and night; Hall & Tank, 2005). The proposed stimulation of ER by either DOC or NO_3^- subsidies could not be confirmed because ER response was not correlated to storm event magnitude or responses in these solutes, suspended solids or GPP. Although ER and solutes on average showed similar delayed responses to storm events, there was no correlation between the event-specific timing of responses. This finding reiterates the limited power of DOC and NO_3^- concentrations for explaining ER event dynamics, warranting further investigation of the effect of DOC quality, pH, redox conditions as well as physical re-organization of benthic communities upon hydrological disturbances. In particular, the lack of correlation between ER and DOC concentration could result from differences in DOC quality across storm events, as labile DOC (either allochthonous or autochthonous) has been identified as a dominant driver of ER (Bertuzzo et al., 2022). Our measured fDOM component (excitation: 365 nm, emission: 480 nm) is characterized by recalcitrant humic substances, which is an appropriate proxy for bulk DOC but does not contain information on labile DOC compounds (Cory & Kaplan, 2012). Thus, to improve our understanding of ER responses to DOC lability, we suggest that monitoring should be complemented with sensors capable of measuring fDOM components corresponding to labile DOC.

5. Conclusions

The increasing availability of high-frequency water chemistry time series and development of robust approaches to model stream metabolism have provided critical insights into in-stream biogeochemical processing of solutes across aquatic biomes. Yet, the understanding of how metabolic activity and biogeochemical processing vary over flow conditions remains limited in headwater streams draining intensively managed agricultural catchments. By integrating stream ecosystem biogeochemistry and hydrology, biological demand in the studied agricultural stream was shown to be inefficient in regulating downstream exports of NO_3^- and DOC. The lack of response in photoautotrophic NO_3^- removal during floodplain inundation further suggests that riparian vegetation rather assimilate NO_3^- from floodplain sediments than from the water column, resulting in a delayed impact on stream NO_3^- concentrations that was not captured by the in-stream metabolic signal. Importantly, we show that in a stream with high annual NO_3^- export, seasonal declines in NO_3^- loads coinciding with peaks of high metabolic activity can give rise to NO_3^--limiting conditions. This emphasizes the crucial role of land use and drainage management for enhancing terrestrial N demand, with the aim of restricting seasonal NO_3^- inputs, rather than focusing efforts only on the in-stream remediation capacity for storing and transforming NO_3^-. Likewise, peaks in metabolic activity can also substantially increase removal rates of DOC, although the more stable supply of DOC prevented heterotrophic carbon limitation in the study stream.

During storm events, the use of established concentration-discharge indices for characterizing metabolic patterns enabled a unified comparison of both solute and metabolic responses. This highlighted the potential role of NO_3^- dilution as a suppression mechanism of GPP during events. It further showed that ER increased consistently during storm events responses during events, but this stimulation could not be directly attributed to either concentrations of NO_3^-, DOC, or to suspended solids. Therefore, novel approaches integrating the effect of DOC quality as well as the physical microbial community structure are needed to better understand what drives ER changes during storms. Our findings assert the importance of including highly impacted systems into the growing body of solute processing capacity of headwaters, further aiding the constraint of biogeochemical flows across stream networks with diverse land use.

Data Availability Statement

Modeled metabolism, solute supply, dissolved O_2 concentrations and hydrology data that support the findings of this study are openly available at the Figshare repository: https://doi.org/10.6084/m9.figshare.25959253 (Hallberg, Bernal, & Bieroza, 2024).

Acknowledgments
This project was funded by Svenska Forskningsrådet Formas (2018-00890), Havs-och vattenmyndigheten (3280-2019), and Oscar och Lili Lamms Minne (DO2019-0021) awarded to M. Bieroza. S. Bernal worked was supported by the projects EVASIONA (PID2021-122817-NB-100) and RIPAMED (CNS2023-144737) from the Spanish Ministry of Science, Innovation, and Universities, AEI/FEDER UE, and Next Generation funding. The authors would like to thank private landowners and stakeholders in the study catchment for their help with collecting water and sediments samples and providing access to field sites, especially Christoffer Bonthron from Tullstorpsåprojektet. We thank Sheryl Illao Åström for conducting the geometrical surveys and compiling GPS data.

References

Abbott, B. W., Gruau, G., Zarnetske, J. P., Moatar, F., Barbe, L., Thomas, Z., et al. (2018). Unexpected spatial stability of water chemistry in headwater stream networks. *Ecology Letters*, *21*(2), 296–308. https://doi.org/10.1111/ele.12897

Alexander, R. B., Boyer, E. W., Smith, R. A., Schwarz, G. E., & Moore, R. B. (2007). The role of headwater streams in downstream water quality. *Journal of the American Water Resources Association*, *43*(1), 41–59. https://doi.org/10.1111/j.1752-1688.2007.00005.x

Almeida, G. H., Boëchat, I. G., & Gücker, B. (2014). Assessment of stream ecosystem health based on oxygen metabolism: Which sensor to use? *Ecological Engineering*, *69*, 134–138. https://doi.org/10.1016/j.ecoleng.2014.03.027

Appling, A. P., Hall, R. O. Jr., Yackulic, C. B., & Arroita, M. (2018). Overcoming equifinality: Leveraging long time series for stream metabolism estimation. *Journal of Geophysical Research: Biogeosciences*, *123*(2), 624–645. https://doi.org/10.1002/2017JG004140

Appling, A. P., & Heffernan, J. B. (2014). Nutrient limitation and physiology mediate the fine-scale (de)coupling of biogeochemical cycles. *The American Naturalist*, *184*(3), 384–406. https://doi.org/10.1086/677282

Arango, C. P., Tank, J. L., Johnson, L. T., & Hamilton, S. K. (2008). Assimilatory uptake rather than nitrification and denitrification determines nitrogen removal patterns in streams of varying land use. *Limnology & Oceanography*, *6*, 2558–2572. https://doi.org/10.2307/40058344

Baattrup-Pedersen, A., Ovesen, N. B., Larsen, S. E., Andersen, D. K., Riis, T., Kronvang, B., & Rasmussen, J. J. (2018). Evaluating effects of weed cutting on water level and ecological status in Danish lowland streams. *Freshwater Biology*, *63*(7), 652–661. https://doi.org/10.1111/fwb.13101

Bernal, S., Cohen, M. J., Ledesma, J. L. J., Kirk, L., Martí, E., & Lupon, A. (2022). Stream metabolism sources a large fraction of carbon dioxide to the atmosphere in two hydrologically contrasting headwater streams. *Limnology & Oceanography*, *67*(12), 2621–2634. https://doi.org/10.1002/lno.12226

Bernal, S., Lupon, A., Wollheim, W. M., Sabater, F., Poblador, S., & Martí, E. (2019). Supply, demand, and in-stream retention of dissolved organic carbon and nitrate during storms in mediterranean forested headwater streams. *Frontiers in Environmental Science*, *7*(60), 1–14. https://doi.org/10.3389/fenvs.2019.00060

Bernhardt, E. S., Savoy, P., Vlah, M. J., Appling, A. P., Koenig, L. E., Hall, R. O., et al. (2022). Light and flow regimes regulate the metabolism of rivers. *Proceedings of the National Academy of Sciences of the United States of America*, *119*(8), e2121976119. https://doi.org/10.1073/pnas.2121976119

Bernot, M. J., Sobota, D. J., Hall, R. O., Mulholland, P. J., Dodds, W. K., Webster, J. R., et al. (2010). Inter-regional comparison of land-use effects on stream metabolism. *Freshwater Biology*, *55*(9), 1874–1890. https://doi.org/10.1111/j.1365-2427.2010.02422.x

Bernot, M. J., Tank, J. L., Royer, T. V., & David, M. B. (2006). Nutrient uptake in streams draining agricultural catchments of the midwestern United States. *Freshwater Biology*, *51*(3), 499–509. https://doi.org/10.1111/j.1365-2427.2006.01508.x

Bertilsson, S., & Jones, J. B. (2003). Supply of dissolved organic matter to aquatic ecosystems: Autochthonous sources. In S. E. G. Findlay & R. L. Sinsabaugh (Eds.), *Aquatic ecosystems: Interactivity of dissolved organic matter* (pp. 26–70). Academic Press. https://doi.org/10.1016/B978-012256371-3/50002-0

Bertuzzo, E., Hotchkiss, E. R., Argerich, A., Kominoski, J. S., Oviedo-Vargas, D., Savoy, P., et al. (2022). Respiration regimes in rivers: Partitioning source-specific respiration from metabolism time series. *Limnology & Oceanography*, *67*(11), 2374–2388. https://doi.org/10.1002/lno.12207

Bieroza, M., Acharya, S., Benisch, J., ter Borg, R. N., Hallberg, L., Negri, C., et al. (2023). Advances in catchment science, hydrochemistry, and aquatic ecology enabled by high-frequency water quality measurements. *Environmental Science & Technology*, *57*(12), 4701–4719. https://doi.org/10.1021/acs.est.2c07798

Bond, N. (2022). *Hydrostats: Hydrologic indices for daily time series data*. CRAN. [code]. Retrieved from https://CRAN.R-project.org/package=hydrostats

Burdon, F. J., Ramberg, E., Sargac, J., Forio, M. A. E., de Saeyer, N., Mutinova, P. T., et al. (2020). Assessing the benefits of forested riparian zones: A qualitative index of riparian integrity is positively associated with ecological status in European streams. *Water*, *12*(4), 1178. https://doi.org/10.3390/w12041178

Burns, D. A., Pellerin, B. A., Miller, M. P., Capel, P. D., Tesoriero, A. J., & Duncan, J. M. (2019). Monitoring the riverine pulse: Applying high-frequency nitrate data to advance integrative understanding of biogeochemical and hydrological processes. *WIREs Water*, *6*(4), e1348. https://doi.org/10.1002/wat2.1348

Burrell, T. K., O'Brien, J. M., Graham, S. E., Simon, K. S., Harding, J. S., & McIntosh, A. R. (2014). Riparian shading mitigates stream eutrophication in agricultural catchments. *Freshwater Science*, *33*(1), 73–84. https://doi.org/10.1086/674180

Butturini, A., Alvarez, M., Bernal, S., Vazquez, E., & Sabater, F. (2008). Diversity and temporal sequences of forms of DOC and NO_3-discharge responses in an intermittent stream: Predictable or random succession? *Journal of Geophysical Research*, *113*(G3). https://doi.org/10.1029/2008JG000721

Chapra, S. C., & Di Toro, D. M. (1991). Delta method for estimating primary production, respiration, and reaeration in streams. *Journal of Environmental Engineering*, *117*(5), 640–655. https://doi.org/10.1061/(ASCE)0733-9372(1991)117:5(640)

Cory, R. M., & Kaplan, L. A. (2012). Biological lability of streamwater fluorescent dissolved organic matter. *Limnology & Oceanography*, *57*(5), 1347–1360. https://doi.org/10.4319/lo.2012.57.5.1347

Covino, T. P., Bernhardt, E. S., & Heffernan, J. B. (2018). Measuring and interpreting relationships between nutrient supply, demand, and limitation. *Freshwater Science*, *37*(3), 448–455. https://doi.org/10.1086/699202

del Giorgio, P. A., & Cole, J. J. (1998). Bacterial growth efficiency in natural aquatic systems. *Annual Review of Ecology and Systematics*, *29*(1), 503–541. https://doi.org/10.1146/annurev.ecolsys.29.1.503

Demars, B. O. L. (2019). Hydrological pulses and burning of dissolved organic carbon by stream respiration. *Limnology & Oceanography*, *64*(1), 406–421. https://doi.org/10.1002/lno.11048

Descy, J.-P., Leporcq, B., Viroux, L., François, C., & Servais, P. (2002). Phytoplankton production, exudation and bacterial reassimilation in the River Meuse (Belgium). *Journal of Plankton Research*, *24*(3), 161–166. https://doi.org/10.1093/plankt/24.3.161

Dodds, W. K., & Oakes, R. M. (2008). Headwater influences on downstream water quality. *Environmental Management*, *41*(3), 367–377. https://doi.org/10.1007/s00267-007-9033-y

Duff, J. H., Tesoriero, A. J., Richardson, W. B., Strauss, E. A., & Munn, M. D. (2008). Whole-stream response to nitrate loading in three streams draining agricultural landscapes. *Journal of Environmental Quality*, *37*(3), 1133–1144. https://doi.org/10.2134/jeq2007.0187

Ensign, S. H., & Doyle, M. W. (2006). Nutrient spiraling in streams and river networks. *Journal of Geophysical Research*, *111*(G4). https://doi.org/10.1029/2005JG000114

Fenchel, T., Blackburn, H., King, G. M., & Blackburn, T. H. (2012). *Bacterial biogeochemistry: The ecophysiology of mineral cycling*. Academic Press.

Frankforter, J. D., Weyers, H. S., Bales, J. D., Moran, P. W., & Calhoun, D. L. (2010). The relative influence of nutrients and habitat on stream metabolism in agricultural streams. *Environmental Monitoring and Assessment*, *168*(1), 461–479. https://doi.org/10.1007/s10661-009-1127-y

Fuß, T., Behounek, B., Ulseth, A. J., & Singer, G. A. (2017). Land use controls stream ecosystem metabolism by shifting dissolved organic matter and nutrient regimes. *Freshwater Biology*, *62*(3), 582–599. https://doi.org/10.1111/fwb.12887

Gibson, C. A., O'Reilly, C. M., Conine, A. L., & Lipshutz, S. M. (2015). Nutrient uptake dynamics across a gradient of nutrient concentrations and ratios at the landscape scale. *Journal of Geophysical Research: Biogeosciences*, *120*(2), 326–340. https://doi.org/10.1002/2014JG002747

Graeber, D., Boëchat, I. G., Encina-Montoya, F., Esse, C., Gelbrecht, J., Goyenola, G., et al. (2015). Global effects of agriculture on fluvial dissolved organic matter. *Scientific Reports*, *5*(1), 16328. https://doi.org/10.1038/srep16328

Hall, R. O., & Beaulieu, J. J. (2013). Estimating autotrophic respiration in streams using daily metabolism data. *Freshwater Science*, *32*(2), 507–516. https://doi.org/10.1899/12-147.1

Hall, R. O., & Tank, J. L. (2005). Correcting whole-stream estimates of metabolism for groundwater input. *Limnology and Oceanography: Methods*, *3*(4), 222–229. https://doi.org/10.4319/lom.2005.3.222

Hallberg, L., Bernal, S., & Bieroza, M. (2024). Data from: Seasonal variation in flow and metabolic activity drive nitrate and carbon supply and demand in a temperate agricultural stream [Dataset]. *Figshare*. https://doi.org/10.6084/m9.figshare.25959253

Hallberg, L., Djodjic, F., & Bieroza, M. (2024). Phosphorus supply and floodplain design govern phosphorus reduction capacity in remediated agricultural streams. *Hydrology and Earth System Sciences*, *28*(2), 341–355. https://doi.org/10.5194/hess-28-341-2024

Hallberg, L., Hallin, S., & Bieroza, M. (2022). Catchment controls of denitrification and nitrous oxide production rates in headwater remediated agricultural streams. *Science of the Total Environment*, *838*, 156513. https://doi.org/10.1016/j.scitotenv.2022.156513

Hedin, J., & Kivivuori, H. (2015). Tullstorpsåprojektet. Utvärdering. Tvåstegsdiken och kantavplaning sträckan Stora Markie-Stävesjö Ålholmens dikningsföretag. Rapport. Naturvårdsingenjörerna AB. https://tullstorpsan.se/rapporter/Tvastegsdiken_och_kantavplaning.pdf

Heffernan, J. B., & Cohen, M. J. (2010). Direct and indirect coupling of primary production and diel nitrate dynamics in a subtropical spring-fed river. *Limnology & Oceanography*, *55*(2), 677–688. https://doi.org/10.4319/lo.2010.55.2.0677

Hill, A. R. (2023). Patterns of nitrate retention in agriculturally influenced streams and rivers. *Biogeochemistry*, *163*(2), 155–183. https://doi.org/10.1007/s10533-023-01027-w

Hoellein, T. J., Bruesewitz, D. A., & Richardson, D. C. (2013). Revisiting Odum (1956): A synthesis of aquatic ecosystem metabolism. *Limnology & Oceanography*, *58*(6), 2089–2100. https://doi.org/10.4319/lo.2013.58.6.2089

Jarvie, H. P., Sharpley, A. N., Kresse, T., Hays, P. D., Williams, R. J., King, S. M., & Berry, L. G. (2018). Coupling high-frequency stream metabolism and nutrient monitoring to explore biogeochemical controls on downstream nitrate delivery. *Environmental Science & Technology*, *52*(23), 13708–13717. https://doi.org/10.1021/acs.est.8b03074

Jarvie, H. P., Smith, D. R., Norton, L. R., Edwards, F. K., Bowes, M. J., King, S. M., et al. (2018). Phosphorus and nitrogen limitation and impairment of headwater streams relative to rivers in Great Britain: A national perspective on eutrophication. *Science of the Total Environment*, *621*, 849–862. https://doi.org/10.1016/j.scitotenv.2017.11.128

Kelly, P. T., Renwick, W. H., Knoll, L., & Vanni, M. J. (2019). Stream nitrogen and phosphorus loads are differentially affected by storm events and the difference may be exacerbated by conservation tillage. *Environmental Science & Technology*, *53*(10), 5613–5621. https://doi.org/10.1021/acs.est.8b05152

King, S. A., Heffernan, J. B., & Cohen, M. J. (2014). Nutrient flux, uptake, and autotrophic limitation in streams and rivers. *Freshwater Science*, *33*(1), 85–98. https://doi.org/10.1086/674383

Lloyd, C. E. M., Freer, J. E., Johnes, P. J., & Collins, A. L. (2015). Technical note: Testing an improved index for analysing storm nutrient hysteresis. *Hydrology and Earth System Sciences Discussions*, *12*(8), 7875–7892. https://doi.org/10.5194/hessd-12-7875-2015

Lumley, T. (2020). *Leaps: Regression subset selection*. CRAN. [code]. Retrieved from https://CRAN.R-project.org/package=leaps

Maynard, J. J., Dahlgren, R. A., & O'Geen, A. T. (2012). Quantifying spatial variability and biogeochemical controls of ecosystem metabolism in a eutrophic flow-through wetland. *Ecological Engineering*, *47*, 221–236. https://doi.org/10.1016/j.ecoleng.2012.06.032

Mebane, C. A., Ray, A. M., & Marcarelli, A. M. (2021). Nutrient limitation of algae and macrophytes in streams: Integrating laboratory bioassays, field experiments, and field data. *PLoS One*, *16*(6), e0252904. https://doi.org/10.1371/journal.pone.0252904

Mineau, M. M., Wollheim, W. M., Buffam, I., Findlay, S. E. G., Hall, R. O. Jr., Hotchkiss, E. R., et al. (2016). Dissolved organic carbon uptake in streams: A review and assessment of reach-scale measurements. *Journal of Geophysical Research: Biogeosciences*, *121*(8), 2019–2029. https://doi.org/10.1002/2015JG003204

Mulholland, P. J. (2004). The importance of in-stream uptake for regulating stream concentrations and outputs of N and P from a forested watershed: Evidence from long-term chemistry records for Walker Branch Watershed. *Biogeochemistry*, *70*(3), 403–426. https://doi.org/10.1007/s10533-004-0364-y

O'Donnell, B., & Hotchkiss, E. R. (2022). Resistance and resilience of stream metabolism to high flow disturbances. *Biogeosciences*, *19*(4), 1111–1134. https://doi.org/10.5194/bg-19-1111-2022

Odum, H. T. (1956). Primary production in flowing waters. *Limnology & Oceanography*, *1*(2), 102–117. https://doi.org/10.4319/lo.1956.1.2.0102

Pastor, A., Holmboe, C. M. H., Pereda, O., Giménez-Grau, P., Baattrup-Pedersen, A., & Riis, T. (2023). Macrophyte removal affects nutrient uptake and metabolism in lowland streams. *Aquatic Botany*, *189*, 103694. https://doi.org/10.1016/j.aquabot.2023.103694

Peterson, B. J., Wollheim, W. M., Mulholland, P. J., Webster, J. R., Meyer, J. L., Tank, J. L., et al. (2001). Control of nitrogen export from watersheds by headwater streams. *Science*, *292*(5514), 86–90. https://doi.org/10.1126/science.1056874

Petrie, A. (2020). *regclass: Tools for an introductory class in regression and modeling*. CRAN. [code]. Retrieved from https://CRAN.R-project.org/package=regclass

Plont, S., O'Donnell, B. M., Gallagher, M. T., & Hotchkiss, E. R. (2020). Linking carbon and nitrogen spiraling in streams. *Freshwater Science*, *39*(1), 126–136. https://doi.org/10.1086/707810

Preiner, S., Dai, Y., Pucher, M., Reitsema, R. E., Schoelynck, J., Meire, P., & Hein, T. (2020). Effects of macrophytes on ecosystem metabolism and net nutrient uptake in a groundwater fed lowland river. *Science of the Total Environment*, *721*, 137620. https://doi.org/10.1016/j.scitotenv.2020.137620

Qian, J., Jin, W., Hu, J., Wang, P., Wang, C., Lu, B., et al. (2021). Stable isotope analyses of nitrogen source and preference for ammonium versus nitrate of riparian plants during the plant growing season in Taihu Lake Basin. *Science of the Total Environment*, *763*, 143029. https://doi.org/10.1016/j.scitotenv.2020.143029

Raymond, P. A., Saiers, J. E., & Sobczak, W. V. (2016). Hydrological and biogeochemical controls on watershed dissolved organic matter transport: Pulse-shunt concept. *Ecology*, *97*(1), 5–16. https://doi.org/10.1890/14-1684.1

Raymond, P. A., Zappa, C. J., Butman, D., Bott, T. L., Potter, J., Mulholland, P., et al. (2012). Scaling the gas transfer velocity and hydraulic geometry in streams and small rivers. *Limnology and Oceanography: Fluids and Environments*, *2*(1), 41–53. https://doi.org/10.1215/21573689-1597669

Redfield, A. C. (1958). The biological control of chemical factors in the environment. *American Scientist*, *46*(3), 230A.

Reichert, P., Uehlinger, U., & Acuña, V. (2009). Estimating stream metabolism from oxygen concentrations: Effect of spatial heterogeneity. *Journal of Geophysical Research*, *114*(G3). https://doi.org/10.1029/2008JG000917

Roley, S. S., Tank, J. L., Griffiths, N. A., Hall, R. O., & Davis, R. T. (2014). The influence of floodplain restoration on whole-stream metabolism in an agricultural stream: Insights from a 5-year continuous data set. *Freshwater Science*, *33*(4), 1043–1059. https://doi.org/10.1086/677767

Roley, S. S., Tank, J. L., Stephen, M. L., Johnson, L. T., Beaulieu, J. J., & Witter, J. D. (2012). Floodplain restoration enhances denitrification and reach-scale nitrogen removal in an agricultural stream. *Ecological Applications*, *22*(1), 281–297. https://doi.org/10.1890/11-0381.1

Royer, T. V., David, M. B., & Gentry, L. E. (2006). Timing of riverine export of nitrate and phosphorus from agricultural watersheds in Illinois: Implications for reducing nutrient loading to the Mississippi River. *Environmental Science & Technology*, *40*(13), 4126–4131. https://doi.org/10.1021/es052573n

Rozemeijer, J. C., van der Velde, Y., van Geer, F. C., Bierkens, M. F. P., & Broers, H. P. (2010). Direct measurements of the tile drain and groundwater flow route contributions to surface water contamination: From field-scale concentration patterns in groundwater to catchment-scale surface water quality. *Environmental Pollution*, *158*(12), 3571–3579. https://doi.org/10.1016/j.envpol.2010.08.014

Seybold, E., & McGlynn, B. (2018). Hydrologic and biogeochemical drivers of dissolved organic carbon and nitrate uptake in a headwater stream network. *Biogeochemistry*, *138*(1), 23–48. https://doi.org/10.1007/s10533-018-0426-1

Speir, S. L., Tank, J. L., & Mahl, U. H. (2020). Quantifying denitrification following floodplain restoration via the two-stage ditch in an agricultural watershed. *Ecological Engineering*, *155*, 105945. https://doi.org/10.1016/j.ecoleng.2020.105945

Tank, J. L., Martí, E., Riis, T., von Schiller, D., Reisinger, A. J., Dodds, W. K., et al. (2018). Partitioning assimilatory nitrogen uptake in streams: An analysis of stable isotope tracer additions across continents. *Ecological Monographs*, *88*(1), 120–138. https://doi.org/10.1002/ecm.1280

Thomas, N. W., Arenas, A. A., Schilling, K. E., & Weber, L. J. (2016). Numerical investigation of the spatial scale and time dependency of tile drainage contribution to stream flow. *Journal of Hydrology*, *538*, 651–666. https://doi.org/10.1016/j.jhydrol.2016.04.055

Trentman, M. T., Hall, R. O. Jr., & Valett, H. M. (2023). Exploring the mismatch between the theory and application of photosynthetic quotients in aquatic ecosystems. *Limnology and Oceanography Letters*, *8*(4), 565–579. https://doi.org/10.1002/lol2.10326

Trentman, M. T., Tank, J. L., Davis, R. T., Hanrahan, B. R., Mahl, U. H., & Roley, S. S. (2022). Watershed-scale land use change increases ecosystem metabolism in an agricultural stream. *Ecosystems*, *25*(2), 441–456. https://doi.org/10.1007/s10021-021-00664-2

von Schiller, D., Martí, E., Riera, J. L., Ribot, M., Marks, J. C., & Sabater, F. (2008). Influence of land use on stream ecosystem function in a Mediterranean catchment. *Freshwater Biology*, *53*(12), 2600–2612. https://doi.org/10.1111/j.1365-2427.2008.02059.x

Webster, J. R., Mulholland, P. J., Tank, J. L., Valett, H. M., Dodds, W. K., Peterson, B. J., et al. (2003). Factors affecting ammonium uptake in streams – An inter-biome perspective. *Freshwater Biology*, *48*(8), 1329–1352. https://doi.org/10.1046/j.1365-2427.2003.01094.x

Wollheim, W. M., Bernal, S., Burns, D. A., Czuba, J. A., Driscoll, C. T., Hansen, A. T., et al. (2018). River network saturation concept: Factors influencing the balance of biogeochemical supply and demand of river networks. *Biogeochemistry*, *141*(3), 503–521. https://doi.org/10.1007/s10533-018-0488-0

Workshop, S. S. (1990). Concepts and methods for assessing solute dynamics in stream ecosystems. *Journal of the North American Benthological Society*, *9*(2), 95–119. https://doi.org/10.2307/1467445

References From the Supporting Information

Myneni, R. B., & Williams, D. L. (1994). On the relationship between FAPAR and NDVI. *Remote Sensing of Environment*, *49*(3), 200–211. https://doi.org/10.1016/0034-4257(94)90016-7

Snyder, L., Potter, J. D., & McDowell, W. H. (2018). An evaluation of nitrate, fDOM, and turbidity sensors in New Hampshire streams. *Water Resources Research*, *54*(3), 2466–2479. https://doi.org/10.1002/2017WR020678

Watras, C. J., Hanson, P. C., Stacy, T. L., Morrison, K. M., Mather, J., Hu, Y. H., & Milewski, P. (2011). A temperature compensation method for CDOM fluorescence sensors in freshwater. *Limnology and Oceanography: Methods*, *9*(7), 296–301. https://doi.org/10.4319/lom.2011.9.296